Hindawi
International Journal of Chemical Engineering
Volume 2018, Article ID 4972070, 10 pages
https://doi.org/10.1155/2018/4972070

Research Article

Pt-Co and Pt-Ni Catalysts of Low Metal Content for H_2 Production by Reforming of Oxygenated Hydrocarbons and Comparison with Reported Pt-Based Catalysts

Liza A. Dosso, Carlos R. Vera, and Javier M. Grau

Instituto de Investigaciones en Catálisis y Petroquímica "Ing. José Miguel Parera" (INCAPE), FIQ, UNL-CONICET, CCT CONICET Santa Fe, "Dr. Alberto Cassano, " Colec. Ruta Nac. No. 168, KM 0, Paraje El Pozo, S3000AOJ Santa Fe, Argentina

Correspondence should be addressed to Javier M. Grau; jgrau@fiq.unl.edu.ar

Received 7 February 2018; Accepted 4 June 2018; Published 11 July 2018

Academic Editor: Eric Guibal

New catalysts of Pt, PtNi, PtCo, and NiCo supported on Al_2O_3 were developed for producing hydrogen by aqueous phase reforming (APR) of oxygenated hydrocarbons. The urea matrix combustion technique was used for loading the metal on the support in order to improve several aspects: increase both the metal-support interaction and the metal dispersion and decrease the metal load. The catalysts were characterized by MS/ICP, N_2 adsorption, XRD, TPR, CO chemisorption, and the test of cyclohexane dehydrogenation (CHD). The APR of a solution of 10% mass ethylene glycol (EG), performed in a tubular fixed bed reactor at 498 K, 22 bar, WHSV = 2.3 h^{-1}, was used as the main reaction test. After 10 h on-stream, the catalysts prepared by UMC had better hydrogen yield and catalytic stability than common catalysts prepared by IWI. The UMC/IWI H_2 yield ratio was 23.5/15.2 for Pt, 24.0/17.0 for PtCo, 26.6/21.0 for PtNi, and 8.0/3.9 for NiCo. Ni or Co addition to Pt increased the carbon conversion while keeping the H_2 turnover high. Cobalt also improves stability. Reports of several authors were revised for a comparison. The analysis indicated that the developed catalysts are a viable and cheaper alternative for H_2 production from a renewable resource.

1. Introduction

Current methods of industrial hydrogen production used in petroleum refineries require high temperatures, about 800 K in the case of naphtha reforming [1] and 1200 K for methane steam reforming [2]. These two processes make use of nonrenewable, fossil fuel raw materials and are carried out in the gas phase (GPR).

Nowadays, a growing need exists for processing heavy crudes with a high content of heteroatoms and polyaromatic molecules. Large amount of hydrogen is needed for the hydrotreatment of biomass-derived oxygenates. Many works about the hydrodeoxygenation of lignin-derived phenolic have been reported [3–5]. This makes the use of extensive hydrocracking, hydrodesulphurization, dearomatization, hydrodeoxygenation, and so on, a common refining and biorefining practice. Alternative sources of hydrogen supply are thus becoming necessary.

The burning of fossil fuels has a major impact on the increase of the concentration of CO_2 in the atmosphere. On the contrast, energy derived from biomass releases carbon with a carbon-energy ratio similar to that of coal. However, as indicated by Wuebbles and Jain [6], biomass has already absorbed an equal amount of carbon from the atmosphere before its emission, and therefore the net carbon emissions of biomass fuels are zero during their life cycle. As explained by Nozawa et al. [7], the production of hydrogen from biorenewable sources is a promising way of minimizing environmental problems associated with the combustion of fossil fuels.

The aqueous phase reforming (APR) of oxygenated hydrocarbons derived from biomass is considered a promising alternative process for supplying great amounts of hydrogen at a conveniently low cost. Biomass reforming also has a neutral CO_2 life cycle, making it convenient from an environmental point of view. APR of oxygenated hydrocarbons

can also be performed at low reaction temperatures, for example, 500 K, thermodynamically favoring hydrogen formation with low carbon monoxide content. An overview of aqueous-phase catalytic processes for production of hydrogen and alkanes in a bio refinery has been shown by Huber and Dumesic [8]. In this sense, APR has been recently considered a promising route to upgrade organic compounds found in bio refinery water fractions [9].

One of the key aspects of the APR technology is the design of a suitable catalyst. Many reports study catalysts based on supported Pt. These reports highlight the influence of the amount of available metal surface on the overall activity and the selectivity to hydrogen. Thus, best-performing catalysts have high Pt surface areas per unit catalyst mass. Due to the difficulties of achieving and maintaining a high metal dispersion, most current Pt catalysts for APR have great Pt loads and high associated costs. One way of reducing the catalyst cost is to partially or totally replace Pt by another transition metal with similar properties. For instance, Ni provides good hydrogen yields in gas phase reforming. However, Davda et al. [10] have reported that the performance of Ni in APR is lower than that of pure Pt and that also Ni suffers from intense sintering.

Shabaker et al. [11] used Raney Ni for APR of oxygenated hydrocarbons and got good catalytic activity. However, preparation and handling of pyrophoric Raney Ni are cumbersome and hazardous. Co is also effective for breaking the C-C bond, key reaction step for the generation of H_2. However, it has too high selectivity to methane, an undesired final product that consumes much of the produced hydrogen [7]. Supported Co catalysts for APR are also unstable and sinter to a great extent. Their selectivity to coke is also high unless used in the form of Co-Pt alloys [12]. Best performing Co catalysts are those having small metal particles of easy reducibility [13]. This high metal dispersion is however difficult to achieve by common preparation techniques.

González-Cortés et al. [14, 15] described an alternative method for dispersing transition metals on Al_2O_3 by means of the coimpregnation of the metal salts with urea, followed by drying and fast calcination (combustion) of the formed urea matrix (UMC method). Combustion forms structural defects on the support that act as additional transition metal anchoring sites [16], increasing the number of metal particles and decreasing their average size. This preparation method reportedly allows the preparation of supported metal catalysts of higher dispersion and lower metal load, decreasing the catalysts fabrication costs.

Another issue is that of the choice of the support. Different groups have obtained catalysts with high hydrogen yields, but they not only use high Pt loads but also use special supports [10]. It would be desirable to use alumina as support since it has an affordable low price and good textural and mechanical properties, such as surface area, pore volume, pore size, crush, and sintering resistance.

Most APR catalysts have high fabrication costs. In this sense, the focus of the present work is put on the comparison of the catalysts of this work, which have relatively low metal content, with those prepared by conventional methods that have been reported in the open literature. The aim is to obtain similar properties as those of these reported catalysts.

The catalytic properties are compared of reference Pt, PtNi, PtCo, and NiCo catalysts supported on alumina, prepared by a classical method (incipient wetness impregnation of the precursor solutions on gamma alumina) with catalysts of similar composition prepared by the UMC technique. Properties studied are activity, hydrogen yield, selectivity, hydrogen turn-over frequency TOF_{H_2}, and stability. Particularly, the stability is assessed by measuring both the velocity of coke fouling during the reaction test and the leaching of the metal phase. The catalytic properties are assessed by means of the reaction of aqueous phase reforming of ethylene glycol. Finally, the properties of the best performing catalysts are compared with the properties of catalysts reported by other authors.

2. Materials and Methods

2.1. Catalyst Preparation. Two different methods were used to incorporate the metals to the support: (i) the common simultaneous incipient wetness impregnation (IWI) of the metal precursors, followed by slow calcination; (ii) the method of simultaneous wet impregnation of the metal precursors with urea, followed by the fast combustion of the urea matrix (UMC) [14, 15, 17]. In both cases, the support used was γ-Al_2O_3 (Sasol Alumina spheres 2.5/210), thermally stabilized for 2 h at 873 K, 0.06 $cm^3 \cdot g^{-1}$ pore volumes, with 208.8 $m^2 \cdot g^{-1}$ specific surface area, and ground to a particle size of 35–80 mesh. Salt metal precursors were Pt $(NH_3)_4(NO_3)_2$, $Ni(NO_3)_2$, and $Co(NO_3)_2$ (all Sigma Aldrich, R.P.A). Aqueous solutions of adequate concentration were prepared and then used in the impregnation, in order to obtain final catalysts with 1% Pt and 3% Ni or Co on a mass basis.

In the case of the IWI route, the support was dried in a stove at 383 K for 12 h after impregnation and was then slowly heated from room temperature to 723 K (10 $K \cdot min^{-1}$), then kept and calcined at this temperature for 3 h in flowing air (30 $cm^3 \cdot min^{-1}$). In the case of the UMC route, a solution was prepared that contained urea and the metal precursors with a ratio of 10 mol urea per mol of metal (all metals). The pH of the solution was adjusted to 7, and then the support was immersed in the solution. The system was stirred gently for 3 h at 323 K. The solution excess was evaporated at 323 K until a slurry was formed, and then it was quickly calcined for 10 min at 773 K [14, 15]. Finally, the oxides formed by both routes were reduced in a stream of hydrogen, 1 h at 773 K in situ, in the same steel tubular reactor used for the reaction test.

Mono and bimetallic catalysts were identified according to the following description: Pt-IWI; PtNi-IWI; PtCo-IWI, NiCo-IWI, Pt-UMC; PtNi-UMC; PtCo-UMC; and NiCo-UMC. The UMC and IWI acronyms indicate the preparation route used.

2.2. Catalyst Characterization. The concentration of the supported metals (Pt, Ni, and Co) in the catalysts was

determined by mass spectroscopy with inductively coupled plasma (MS/ICP). The equipment used was an ARL 3410 with argon as gas for the plasma. The solid sample was dissolved in a sulphuric acid solution (50% vol.), and then an aliquot was placed in the nebulizer of the ICP, and the concentration of the metal cations was determined from the mass spectrum of the ion source, as measured by means of a quadrupole mass spectrometer.

The concentration of exposed metal sites was determined using CO as a molecular probe. CO selectively chemisorbs on the surface metal atoms of the metal particles. For this test, an amount of 0.05 g of reduced catalyst was used. Calibrated pulses of a $CO : N_2$ mixture (1.46% CO in N_2, molar basis) were sent to the reactor cell until the metallic surface became saturated. The nonadsorbed CO was converted to CH_4 with H_2 over a Ni/Kieselguhr catalyst and detected by a flame ionization detector connected to the exhaust of the reactor. The adsorbed CO was determined from a mass balance.

The specific surface area was measured in a volumetric system from the N_2 adsorption isotherm obtained at 77 K. The specific surface area (BET method) and porosity measurements were performed in a model ASAP 2020 Micromeritics apparatus using 0.3 g of sample. Samples were outgassed by heat under vacuum ($1.333\,10^{-9}$ bar) at 523 K for 30 h before the nitrogen adsorption.

X-ray diffraction tests were performed in an XD-D1 Shimadzu diffractometer. A sample of about 0.3 g was dried in an oven and then ground to a powder. Then, it was placed on a sample holder and irradiated with Cu Kα monochromatic radiation of a wavelength of about 1.54 Å, filtered with Ni, and operated at 40 kV and 40 mA, at a scan rate of $2^\circ\,\text{min}^{-1}$ and scanning the 20–80° 2θ range.

The temperature-programmed reduction technique (TPR) allows the study of the reducibility of the surface species on the solid support and the degree of interaction between them, especially metal-metal, metal-promoter, and metal-support interactions. Reducibility was measured by H_2 consumption as the sample was subjected to a heating schedule. An Ohkura TP 2002s equipment with a thermal conductivity detector (TCD) was used for these experiments. A known mass of catalyst was first treated in flowing air at 723 K for 1 h and then brought to room temperature. Then the sample was flushed with flowing Ar for 15 min, and the reducing mixture (5% H_2 in Ar) was passed over the sample at room temperature. Once the system was stabilized, the temperature was raised linearly from room temperature to 973 K at a heating rate of $10\,\text{K}\,\text{min}^{-1}$.

2.3. Catalytic Activity Tests. The cyclohexane dehydrogenation (CHD) reaction test allows evaluating the metallic phase of the catalyst. This reaction is known to proceed with a rate that is strictly proportional to the number of surface metal sites, with no regards to metal particle size or surface atom location. This means this reaction is not sensitive to the catalyst structure [18]. The reaction was performed in a glass reactor. The catalyst mass used was 0.1 g, the reaction temperature 573 K, pressure 1 bar, hydrogen flow rate $80\,\text{cm}^3\cdot\text{min}^{-1}$, and cyclohexane flow rate $1.61\,\text{cm}^3\cdot\text{h}^{-1}$ (99.9% Merck). Before the reaction, the catalyst was reduced at 773 K for 1 h with hydrogen. The products were analyzed on-line in a gas chromatograph, with a copper capillary column 100 m long, 0.5 mm internal diameter, and a squalene coating phase.

Aqueous-phase reforming of ethylene glycol was performed in a tubular stainless steel AISI 316L reactor of 9.5 mm internal diameter and of 1.5 mm thickness, heated by an electric oven. The system had a similar configuration as that used by Shabaker et al. [11]. In the experiments, a mass of 0.5 g of catalyst was previously reduced in situ at 773 K for 1 h in hydrogen flow. Then the system was purged with He, and the reaction pressure was adjusted to the desired value by means of a back pressure regulator. The feed, an aqueous solution of ethylene glycol (10%, mass basis), was injected to the reactor by an HPLC pump at a flow rate of $0.02\,\text{cm}^3\cdot\text{min}^{-1}$. The reaction was performed at 498 K, 22 bar, $\text{WHSV} = 2.34\,\text{h}^{-1}$ ($\text{LHSV} = 0.86\,\text{h}^{-1}$). The reaction temperature and pressure were controlled to a narrow margin (±5 K, ±0.1 bar). The products of the reaction were cooled down in a condenser connected on-line and downstream the reactor. The flow rate of the exit gases was $3\,\text{cm}^3\cdot\text{min}^{-1}$. The gases were analyzed on-line with a Shimadzu 8A gas chromatograph using a thermal conductivity detector and a Restek Shin Carbon Micropacked ST column. Total time-on-stream was 10 h. Yields to hydrogen, methane, and other products were determined from compositional data, according to the following formula [10]:

$$H_2 \text{ yield} = \frac{H_2 \text{ in the gas products}}{H_2 \text{ theoretically calculated}} \times 100. \quad (1)$$

This is not the common definition of yield but is that used by Dumesic and coworkers. It has been adopted here for the sake of comparison. "H_2 *in the gas products*" is the molar hydrogen flow rate measured at the reactor outlet. As no hydrogen is fed to the reactor, this is equal to the hydrogen produced. "H_2 *theoretically calculated*" is the hypothetical hydrogen flow rate produced if all the EG feedstock was reformed according to

$$C_2H_6O_2 \longleftrightarrow 2CO + 3H_2 \quad \text{(ethylene glycol reforming)} \quad (2)$$

$$2CO + 2H_2O \longleftrightarrow 2CO_2 + 2H_2 \quad \text{(water gas shift)} \quad (3)$$

For calculation both (2) and (3) are considered to be irreversible.

$$\text{Conversion}_{\text{C to gas}} = \frac{\text{C in the gas products}}{\text{C fed to the reactor}} \times 100,$$
$$H_2 \text{ selectivity} = \frac{H_2 \text{ in the gas products}}{\text{C in the gas products}} \times \frac{1}{R} \times 100, \quad (4)$$

where R is the H_2/CO_2 ratio for the reforming, equal to 5/2 for ethylene glycol.

Selectivity to carbon products (CP) in the gas products (CO, CO_2, CH_4):

$$\text{CP selectivity} = \frac{\text{CP in the gas products}}{\text{C fed to the reactor}} \times 100. \quad (5)$$

Other parameter calculated was the turn-over frequency for hydrogen production (TOF_{H_2}), in units of mols of H_2 per unit time and surface metal site. For calculating the rates of H_2 formation expressed as TOF_{H_2}, the number of surface metal sites was assumed to be equal to the amount of CO molecules irreversibly chemisorbed at 300 K. This is also the treatment used by Davda et al. [19].

$$TOF_{H_2} = \frac{H_2 \text{ in the gas product}}{\text{CO chemisorbed on surface metal atoms} \times \text{min}}. \quad (6)$$

2.4. Deactivation Study. The stability of the APR catalytic system is limited by three main factors: fouling by coke, sintering, and leaching of the metallic phase. The deactivation by coking was assessed by temperature programmed oxidation (TPO) of the coke deposit of the spent catalysts. An amount of 0.05 g of deactivated catalyst was first loaded into a quartz reactor, and then an oxidizing gas mixture (2% O_2 in N_2, molar basis, 30 $cm^3 \cdot min^{-1}$ flow rate) was forced through the sample. The reactor was heated at a rate of 10 $K \cdot min^{-1}$ from room temperature up to 973 K. In the presence of oxygen, the deposits were combusted to CO and CO_2. Both gases were transformed into methane over a Ni/kieselguhr catalyst in a methanation reactor and then sent to a flame ionization detector. The TPO trace was thus obtained by registering the FID voltage as a function of the cell temperature. The area under the signal is proportional to the amount of deposited coke. The sintering of the metal phase affects directly the WGS reaction, and it was indirectly assessed by the hydrogen yield obtained at a fixed reaction time. The leaching of active sites was determined by chemical analysis of the used catalyst at the end of each experiment. The analysis was performed by inductively coupled plasma with mass spectroscopy detection (ICP-MS).

To compare the stability of the catalysts, the fouling deactivation rate (after a stabilization period of 3 h) and leaching deactivation rate were calculated as follows:

$$r_{df}\left(\frac{g_{coke}}{100 g_{cat} \cdot h}\right) = \frac{\%\left(\text{Coke}_T\right]_{t_f} - \text{Coke}_T\right]_{t_s}\right)}{\left(t_f - t_s\right)},$$
$$r_{dl}\left(\frac{g_{metal\ leached}}{100 g_{cat} \cdot h}\right) = \frac{\%\left(\text{Metal}_T\right]_{t_i} - \text{Metal}_T\right]_{t_f}\right)}{\left(t_f - t_i\right)}, \quad (7)$$

where $\%\text{Coke}_T]_t$ is the percentage of accumulated coke on catalyst and $\%\text{Metal}_T]_t$ is the percentage of total metal charge on catalyst after t hours on-stream. t_i is the initial reaction time, 0 h; t_s is the stabilization time, 3 h; and t_f is the final reaction time.

2.5. Literature Data Comparison. The technology of aqueous phase reforming (APR) has been specially developed by Randy Cortright and James Dumesic of the University of Wisconsin [20]. Their first pioneering works indicated that it was possible to convert carbohydrates (ethylene glycol, sorbitol, fructose, etc.) in aqueous solution to hydrogen and nonoxygenated hydrocarbons by means of suitable heterogeneous catalysts and relatively mild reaction conditions. These papers were followed by intensive work by other groups. Most catalysts studied had noble metals, for example, Pt, in high loads.

In order to make a comparison, a literature survey was made and data collected related to APR over Pt/Al_2O_3 catalysts. Catalysts with a similar or higher loading of metal phase were considered (in comparison with the catalysts of this work). Data were also collected corresponding to APR catalysts that used similar metal contents but different supports.

3. Results and Discussion

3.1. Catalysts Characterization. Table 1 shows some properties of the metal function of the catalysts: chemical composition, CO chemisorption capacity, reducibility (hydrogen consumption in the TPR experiment), and activity in cyclohexane dehydrogenation (CHD). This table also shows values of specific area of the catalysts after their final activation.

It can be seen that the Ni, Co, and Pt mass contents are similar to the nominal contents. The metal charge does not substantially modify the specific surface of the catalysts. Nitrogen adsorption measurements indicate that the BET surface area of the catalysts varies no more than 8% in comparison to the original value of the metal-free support. The metal addition step is then supposed to occur without blocking of the pore mouths of the catalysts. This points out to a high efficiency of both methods (UMC and IWI) for loading the metals to the support, with negligible loss of metal mass or support-specific area. The results of chemisorption of CO have double importance. First, the CO chemisorption capacity is proportional to the dispersion of the metal. Secondly, CO adsorption is the first step for the water gas shift reaction that results in an increased production of hydrogen. The results indicate that the monometallic Pt catalysts, prepared either by IWI or UMC, have the highest capacity for CO chemisorption, that is, the highest metal particle dispersion. The CO chemisorption capacity of the bimetallic PtNi and PtCo catalysts is lower than the capacity of the monometallic Pt catalysts. The order of CO chemisorption capacity of the catalysts is Pt > PtCo > PtNi. These results coincide with the reports of Ko et al. [21] which indicate that the addition of Ni to Pt/Al_2O_3 catalysts decreases the number of accessible sites for CO adsorption, though it improves the activity for preferential CO oxidation in the presence of H_2. The CO chemisorption capacity of the NiCo-UMC catalysts is similar to that of the monometallic Pt catalysts, but the metal concentration of the latter is six times greater. On the contrast, if we observe the effect of the technique of incorporation of the metal, it is confirmed that in the case of the bimetallic catalysts prepared by UMC, an increase of dispersion of 40 and 45% (capacity of CO chemisorption) is obtained. The dehydrogenation capacity of each catalyst, as

Table 1: Chemical composition, CO chemisorption, H_2 consumption in TPR test, and specific surface area (Sg).

Catalyst	Pt (%)	Co (%)	Ni (%)	μmol CO/g_{cat}	μmol H_2/g_{cat}	Sg (m^2/g)	$Conversion_{CH\ to\ Bz}$ (%)
Pt-IWI	0.98	—	—	48.7	335.1	215	93.4
Pt-UMC	0.99	—	—	49.4	460.8	210	95.4
PtCo-IWI	1.02	3.05	—	25.0	496.8	193	67.3
PtCo-UMC	0.97	2.87	—	34.0	846.1	201	79.1
PtNi-IWI	1.01	—	3.10	18.6	668.4	200	52.0
PtNi-UMC	0.99	—	2.96	27.1	803.9	206	79.5
NiCo-IWI	—	3.05	2.95	35.2	755.4	197	20.3
NiCo-UMC	—	2.99	2.87	50.9	993.1	192	34.1

Cyclohexane to benzene conversion ($Conversion_{CH\ to\ Bz}$) after 1 h on-stream in a dehydrogenation test.

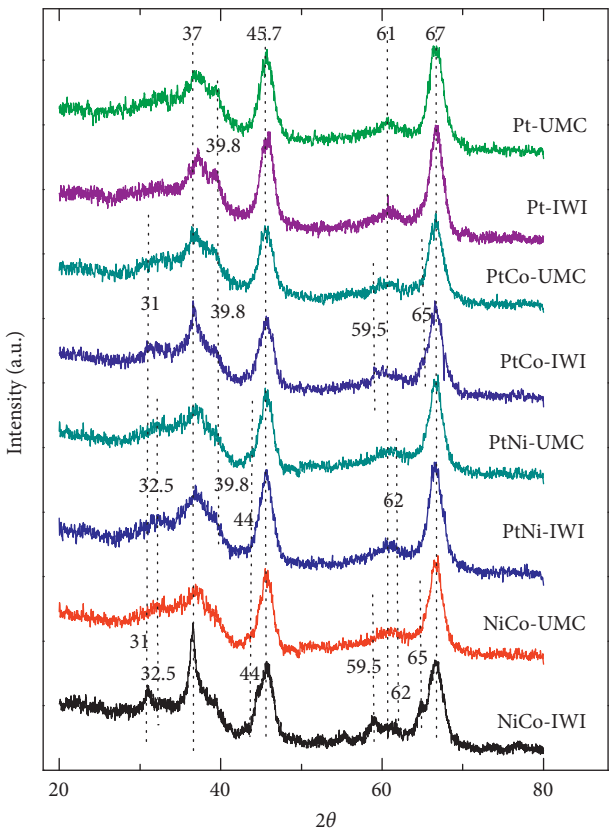

Figure 1: X-ray diffractograms of the studied catalysts.

indicated by the conversion of CH to benzene, is proportional to its CO adsorption capacity. However, its increase is higher for the catalysts containing Pt. For catalysts with the same metal load, the higher the amount of CO chemisorbed, the higher the conversion of cyclohexane. Finally Table 1 also shows values of the consumption of H_2 during the temperature-programmed reduction tests. Bimetallic catalysts have a higher consumption than the monometallic Pt, indicating the coreduction of Ni or Co atoms together or with Pt in each case.

The X-ray powder diffraction patterns of the prepared catalysts are shown in Figure 1.

We can see that all catalysts exhibited the peaks of gamma alumina at 2θ angles of 37°; 39.2°; 45.7°; 61°, and 67° (Joint Committee on Powder Diffraction Standards (JCPDS)) [22]. Low metal loads make it difficult to see bigger differences. If we expand the scale, we can observe that all catalysts that contain Pt show differences at angles of 39.8°, a peak associated to metallic (zero-valent) platinum [23]. These modifications are more remarkable for the catalysts prepared by IWI than those prepared by UMC, indicating a higher size of the metal crystals, that is, a smaller dispersion. For the NiCo-UMC sample, with 3% Ni and 3% Co, small signals of NiO and $NiAl_2O_4$ are observed at 32.5°, 44°, and 62°, and there are no peaks indicating the presence of cobalt oxides [24]. This points to cobalt being in high dispersion or in strong interaction with Ni or with the support. The same catalyst prepared by IWI, NiCo-IWI, shows new peaks at 31°, 59.5°, and 65°, corresponding to Co_3O_4 and $CoAl_2O_4$. The same occurs in the case of the PtCo-IWI catalyst. In addition to the peak corresponding to Pt^0, other signals appear that correspond to cobalt oxides and cobalt aluminate [24]. The XRD spectrum is an evidence of the high degree of dispersion, the strong interaction between metals, or the strong metal-support interaction, in the catalysts prepared by the UMC technique.

TPR traces of the tested catalysts can be seen in Figure 2. The Pt-IWI catalyst has peaks at 500 K and at 680 K while the Pt-UMC catalyst has peaks at 435 K, 500 K, and 680 K. Peaks at temperatures over 640 K are related to Pt species with strong support interaction, like Pt_xAlO_x or Pt_3Al [25]. On the contrast, the 435 K peak of the Pt-UMC catalyst could be related to PtO_x species of low interaction with the support surface [26]. In the case of the PtCo-IWI and PtCo-UMC catalysts, peaks at temperatures below 475 K can be found that could be related to the reduction of Pt species. The shift of the peaks in comparison to the reduction of monometallic Pt could be due to the interference of Co ions. Hydrogen consumption in the region around 300–773 K has been attributed to the reduction of cobalt oxide, as Co_3O_4, along with the reduction of Co^{+3} surface ions [27]. The increase of the size of the first Pt reduction peak could thus be due to the coreduction of Co and Pt species. Above 570 K, the H_2 consumption is related to the reduction of cobalt oxide (Co_3O_4), which involves the reduction of Co_3O_4 to CoO occurring at around 609–640 K. The shift to lower temperatures could be related to H_2 spillover over Pt. Neither PtCo-IWI nor PtCo-UMC has peaks above 1100 K, and a peak appears at 778 K. This means that there are Co species with very high support interaction [28, 29]. As in the case of the monometallic Pt catalyst, the bimetallic catalyst prepared by UMC had a shift of the Pt reduction peak to lower temperatures, indicating the presence of smaller particles.

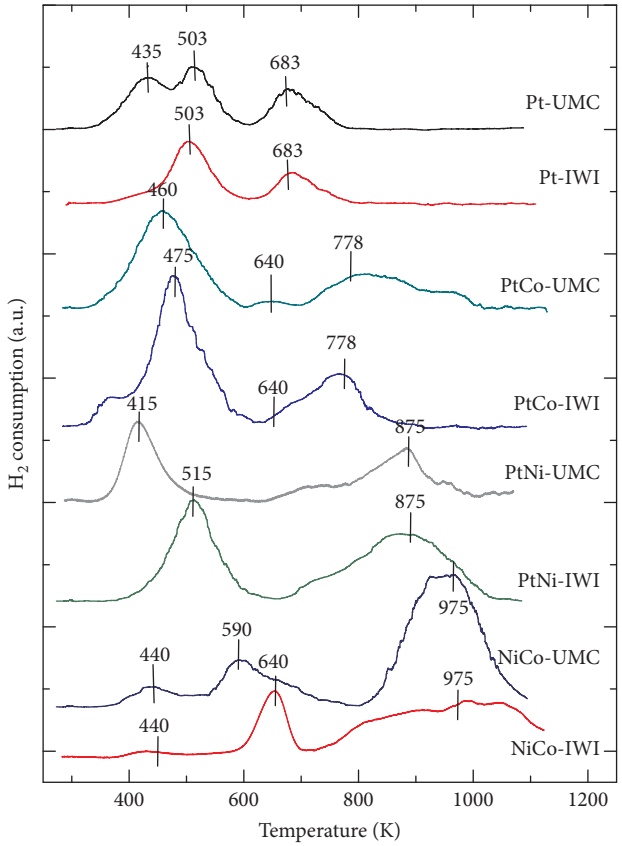

Figure 2: TPR traces of the tested catalysts.

For the PtNi-IWI and PtNi-UMC catalysts, two different peaks are seen. The first one, located at 415–515 K could be related to the reduction of PtOx species interacting with the oxygen atoms of Al_2O_3 and NiO, reduced by the spillover effect of H_2 over Pt. In the catalyst prepared by UMC, a shift to lower temperatures in the reduction peak of Pt species is found. On the contrast, the peak at 875 K is related to the reduction of nickel species. This could be NiO weakly interacting with the Al_2O_3 support ($T < 820$ K) or nickel aluminates, also reduced by the dissociation of H_2 to H• on Pt that penetrated into alumina and reduced more nickel at lower temperatures [30]. The lack of reduction peaks at temperatures above 1000 K could indicate the absence of Ni species with strong interaction with the support as a consequence of the promotion of the reduction of nickel oxides through hydrogen spillover on Pt [31].

The TPR traces of NiCo-IWI and NiCo-UMC catalysts had peaks at 440 K, 590–640 K, and 975 K. Reduction peaks at temperatures below 773 K are related to the reduction of nickel and cobalt ions to metallic Ni and Co. It is suggested by Nabgan et al. [32] that the 975 K peak corresponds to the reduction of a Ni-Co phase in high interaction with the Al_2O_3 support. In the catalyst obtained by UMC, a shift of the intermediate reduction peak is again found.

Summarizing the characterization results, we can observe that for the same metal loading, the UMC technique permits obtaining catalysts with a higher CO-chemisorption capacity, with more dispersed metal particles and with a greater specific area. A higher metal activity for

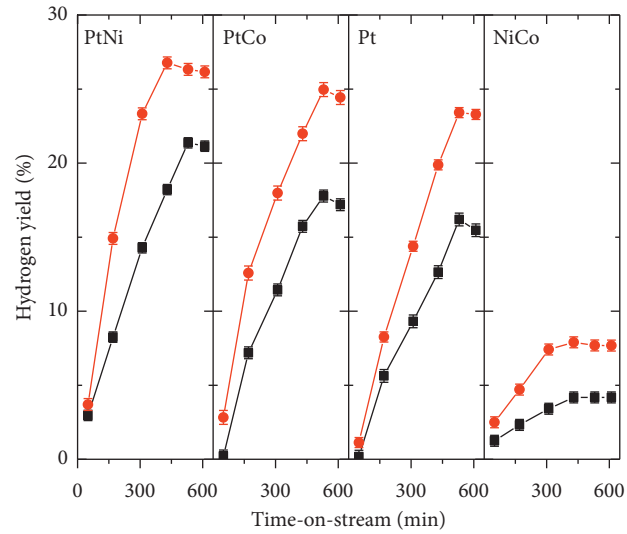

Figure 3: Hydrogen yield of the different catalysts. APR of ethylene glycol (10% aqueous solution). Fixed bed reactor, 498 K 22 bar, WHSV = 2.34 h^{-1}, LHSV = 0.86 h^{-1}. • UMC; ■ IWI.

dehydrogenation was also obtained. These results would confirm the possibility of obtaining catalysts of similar catalytic performance but with lower noble metal concentration.

3.2. Catalytic Properties in APR of Ethylene Glycol. A plot of the hydrogen yield as a function of time-on-stream can be seen in Figure 3. The hydrogen production has an induction period of 6–8 h, and then it stabilizes to almost constant values. The order of hydrogen yield is PtNi-UMC > PtCo-UMC ≈ Pt-UMC > PtNi-IWI > PtCo-IWI ≈ Pt-IWI > NiCo-UMC > NiCo-IWI. It can be seen that the Pt catalyst prepared by the classical IWI technique displays one of the lowest hydrogen yield values.

The numerical results of the catalytic properties at the end of the run indicate (Table 2) that the highest hydrogen selectivity is that of the monometallic Pt catalysts. However, the catalytic conversion on these catalysts is not so high and therefore the hydrogen yield is not the highest.

The total time-on-stream of the APR tests was 10 h. On average PtNi-UMC, PtCo-UMC, and Pt-UMC had higher H_2 yields and TOF_{H2} than Pt-IWI. The catalyst PtNi-UMC had the best hydrogen yield. PtCo-UMC had better yields up to 400 min of time-on-stream, its activity level then becoming similar to that of Pt-UMC. All catalysts show growing hydrogen yields along the run, then stabilizing after 500 min on-stream. This is coincident with the report of Luo et al. [24]. Their catalysts had a stable activity after 10 h on-stream. Afterwards a drop in conversion was registered.

It can also be seen that once the catalysts reach a pseudo steady state, the hydrogen yield values become higher than that of the Pt-IWI catalyst. The difference is 50% for Pt-UMC and PtCo-UMC and 75% for PtNi-UMC. Also for an equal yield to hydrogen, the PtCo-UMC catalyst has a lower selectivity to methane than the Pt-UMC catalyst. Bimetallic PtNi catalysts are the most active and show the highest

Table 2: Results of APR of aqueous ethylene glycol (10% w).

Catalyst	Conversion$_{C\ to\ gas}$, (%)	Selectivity (%)		H_2 yield (%)	TOF_{H_2} (min^{-1})
		CH_4	H_2		
Pt-IWI	42.9	2.0	35.4	15.2	1.01
Pt-UMC	65.0	1.7	36.2	23.5	1.53
PtCo-IWI	64.0	0.7	26.6	17.0	2.19
PtCo-UMC	86.0	0.6	27.9	24.0	2.27
PtNi-IWI	80.0	6.7	26.3	21.0	3.13
PtNi-UMC	86.0	4.6	30.9	26.6	3.16
NiCo-IWI	24.0	11.4	16.3	3.9	0.36
NiCo-UMC	48.0	12.7	16.7	8.0	0.51

Results at 10 h on-stream. Reaction conditions: 498 K, 22 bar, WHSV = 2.34 h^{-1}, and LHSV = 0.86 h^{-1}.

Table 3: Stability of the catalysts in APR of aqueous ethylene glycol (10%w).

Catalyst	$Metal_T]_t$ (%)		$10^4 \times r_{dl}$ ($g_{metal}/g_{cat} \cdot h$)	$Coke_T]_t$ (%)		$10^4 \times r_{df}$ ($g_{coke}/g_{cat} \cdot h$)
	0 h	10 h		3 h	10 h	
Pt-IWI	0.98	0.97	0.1	1.3	1.9	8.6
Pt-UMC	0.99	0.98	0.1	0.9	1.2	4.3
PtCo-IWI	4.07	4.01	0.6	1.2	1.4	2.8
PtCo-UMC	3.84	3.82	0.2	1.1	1.2	1.4
PtNi-IWI	4.11	4.03	0.8	2.8	3.6	11.4
PtNi-UMC	3.95	3.90	0.5	2.8	3.4	8.6
NiCo-IWI	6.00	5.92	0.8	2.4	3.4	14.3
NiCo-UMC	5.86	5.83	0.3	2.5	2.7	2.9

Reaction conditions: 498 K, 22 bar, WHSV = 2.34 h^{-1}, LHSV = 0.86 h^{-1}, and TOS = 10 (h); $Metal_T]_t$: total metal content on coke-free catalyst at (t) hour on-stream; $Coke_T]_t$: coke deposited on the catalyst at (t) hour on-stream; r_{dl}: leaching deactivation rate; r_{df}: fouling deactivation rate.

values of TOF_{H2}. However, their selectivity to methane is high, that is, they consume part of the H_2 produced.

Table 3 shows the percentages of total metal deposited in each catalyst before and after a period of 10 h of reaction and the amounts of carbon deposited on the catalysts after 3 h and 10 h on-stream. From these data, the rates of deactivation by leaching of the metal phase and fouling by coke are calculated.

Regarding leaching, although the variations of the results are within the experimental error of the analysis technique, there is a trend that confirms a stronger anchorage of the metallic particles in the catalysts prepared by UMC with respect to those obtained by the conventional IWI technique. Regarding fouling, the Pt-UMC and the PtCo-UMC catalysts had the lowest coke content. Coke content was below 2% after 10 h on-stream. Pt-UMC had the lowest amount of coke at 3 h on-stream. The Ni-containing catalysts had the highest amount of coke at short and long reaction times. For any of the catalysts, not less than 60% of the total coke was formed in the first 3 h of reaction. This indicates that after the catalyst is stabilized, the coking reactions become slower, probably because of deactivation of the sites of higher coking activity.

After 3 h of reaction, the coke on the metal is stabilized, and the deactivation rate due to fouling is minimal in the samples promoted with cobalt, both in PtCo and in NiCo. The fouling rate increases in the samples with nickel. This trend is more pronounced in the catalysts prepared by UMC.

Figure 4 shows the coke oxidation profiles of the catalysts after 10 h on-stream in the APR test.

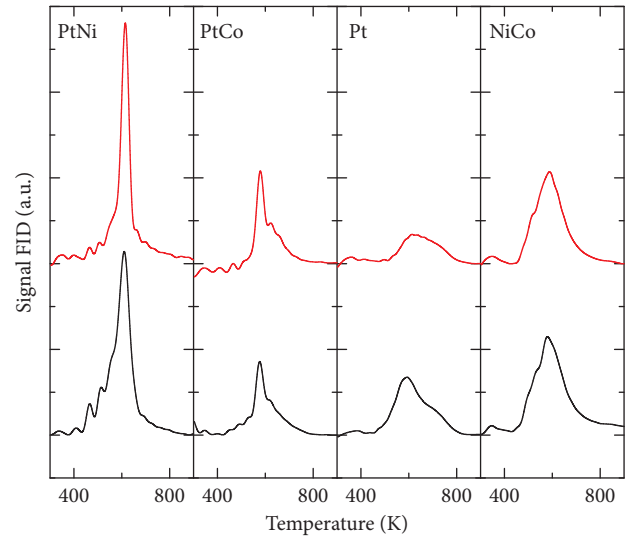

Figure 4: Temperature-programmed oxidation traces of different catalysts. Catalyst coked during a test of 10 h (APR of aqueous ethylene glycol, 10%). – UMC; – IWI.

It can be seen in all cases that coke is burned at temperatures lower than 873 K. The incorporation of Ni into Pt generates a more hydrogenated deposit giving a very sharp coke burning peak. Despite having accumulated the largest amount of coke, its steady-state activity is the largest. The incorporation of Co to Pt reduces the amount of coke and reduces the degree of polymerization, coke being eliminated in a lower temperature range. If we compare the coke

Table 4: Results of APR of ethylene glycol over different catalysts.

Catalyst	EG (% w)	T (K)	P (bar)	WHSV (h^{-1})	LHSV (h^{-1})	Conversion C to gas (%)	Selectivity (%)		H_2 yield (%)	TOF_{H_2} (min^{-1})	Reference
							C_5^-	H_2			
$Pt(3)/Al_2O_3$	1	498	29.3		0.6	90.0	4.0	96.0	86.4	5.3	Shabaker et al. [11]
R-Ni(14)Sn	1	498	25.8		5.1	93.0	4.0	95.0	88.4	1.4	Shabaker et al. [11]
Pt(1)	10	498	29.3		72.0	5.4	1.2	87.1	4.7	1.9	Huber et al. [12]
Pt(1)Ni(1)	10	498	29.3		70.2	5.9	0.0	91.0	5.4	5.2	Huber et al. [12]
Pt(1)Ni(5)	10	498	29.3		138.5	3.6	0.9	89.5	3.2	3.0	Huber et al. [12]
Pt(1)Ni(8)	10	498	29.3		128.6	3.5	2.0	90.2	3.2	2.8	Huber et al. [12]
Pt(1)Co(5)	10	498	29.3		57.4	8.4	0.5	88.2	7.4	5.1	Huber et al. [12]
$Pt(1.5)/Al_2O_3$	1	548	200.0	1.2		78	0.3				De Vlieger et al. [33]
$Pt(1.5)/Al_2O_3$	20	723	250.0	12		74	16.9				De Vlieger et al. [33]
Ni(19)/SiO2	10	498	22.0		n/r	2.3	13.0	57.0	1.3	14.0	Davda et al. [19]
$Pd(5)/SiO_2$	10	498	22.0		n/r	3.1	0.0	98.5	3.0	30.0	Davda et al. [19]
$Pt(6)/SiO_2$	10	498	22.0		n/r	21.0	13.0	77.9	16.4	275.0	Davda et al. [19]
$Ru(6)/SiO_2$	10	498	22.0		n/r	42.0	58.0	7.0	2.9	20.0	Davda et al. [19]
Pt(1)/CMK-3	10	523	45.6	2.0		25.4	4.5	n/r	26.6	103	Kim et al. [38]
Pt(3)/CMK-3	10	523	45.6	2.0		46.0	n/r	n/r	49.3	46.4	Kim et al. [36]
Pt(7)/CMK-3	10	523	45.6	2.0		69.8	7.1	n/r	72.1	31.2	Kim et al. [35]
Pt(3) CMK-9	10	523	45.6	2.0		44.9	4.2	n/r	49.3	n/r	Kim et al. [37]
Fe(3) CMK-9	10	523	45.6	2.0		12.1	8.9	n/r	27.1	n/r	Kim et al. [37]
Pt(3)Fe(3) (1 : 1)	10	523	45.6	2.0		60.8	3.3	n/r	64.9	n/r	Kim et al. [37]
Pt(3)Fe(6) (1 : 2)	10	523	45.6	2.0		63.2	3.1	n/r	66.7	n/r	Kim et al. [37]
Pt(3)Fe(9) (1 : 3)	10	523	45.6	2.0		68.4	2.8	n/r	71.1	~70-80	Kim et al. [37]
Pt(3)Fe(12) (1 : 4)	10	523	45.6	2.0		60.1	2.6	n/r	70.7	n/r	Kim et al. [37]
Pt(3)Fe(15) (1 : 5)	10	523	45.6	2.0		58.9	2.7	n/r	68.8	n/r	Kim et al. [37]

Steady state conditions, fixed bed reactor.

deposits obtained on catalysts of the same composition but synthesized by different methods, a reduction of the coke content on the UMC catalysts can be seen. The degree of metal dispersion obtained by each preparation route evidently modifies the stability of the catalyst.

3.3. Comparison of These Results with Those Obtained by Other Research Groups. In 2002, the group of Professor Dumesic of the University of Wisconsin developed a catalytic process that generated H_2 from the aqueous-phase reforming (APR) of biomass-derived oxygenated compounds such as methanol, ethylene glycol, glycerol, sugars, and sugar-alcohols [20]. Davda et al. [19] tested some Group VIII metals for the APR of 10% ethylene glycol at 483 and 498 K and at a total pressure of 22 bar. They found that the overall catalytic activity for ethylene glycol reforming, as measured by the rate of CO_2 production at 483 K, decreased in the following order for silica-supported metals: Pt~Ni > Ru > Rh~Pd > Ir. Silica supported Rh, Ru, and Ni showed a low selectivity for production of H_2 and a high selectivity for alkane production. In addition, Ni/SiO_2 showed significant deactivation at the higher temperature of 498 K. Silica-supported Pt and Pd catalysts exhibited relatively high selectivities for production of H_2, with low rates of alkane production. It seemed evident that catalysts based on Pt and Pd were promising materials for the selective production of hydrogen.

We can see in Table 4 a summary of results of the APR of solutions of ethylene glycol of varying concentration, at varying temperature, pressure, and flow rate conditions, as published by different authors.

Shabaker et al. [11] reported results of the aqueous phase reforming of solutions of 1% ethylene glycol using an industrial Raney NiSn catalyst and a Pt/Al_2O_3 catalyst with 3% Pt. While conversion and yield to hydrogen were quite high, the selectivity to alkanes was too high, almost 4% for both catalysts. Huber and Dumesic [12] reported results corresponding to a catalyst of 3% Pt on alumina for the APR of aqueous ethylene glycol (10%). Included in the table are also the results corresponding to bimetallic PtNi and PtCo catalysts and metal atomic ratios 1 : 1, 1 : 5, and 1 : 8 (Pt/second metal). None of the catalysts had a conversion above 10% even after reaching the steady state. Supported Pt catalysts over alumina had better results when the reaction conditions were modified [33]. Table 4 shows the conversion results of APR of ethylene glycol over a Pt/Al_2O_3 catalyst with 1.5% Pt. Although the conversion to gas was high, it was necessary to increase the reaction pressure by one order of magnitude. This involves a rise of operation costs. Results for other metals and supports can be inspected in Table 4 [19]. It can be seen that Ni and Pd loaded catalysts have low conversion values when supported on silica, even at high metal loadings, while Pt, Ru, and Rh give high values of conversion but a poor selectivity to hydrogen. This combines with a high selectivity to alkanes to produce a final high selectivity to alkanes and a low hydrogen yield.

Recent studies on Pt supported over carbon nanotubes for the aqueous phase reforming of ethylene glycol showed that the activity can be greatly improved by changing the support to

a more convenient one [34, 35]. However, increasing the catalyst activity threefold demands increasing the metal concentration seven times. We can see in Table 4 that though the activity level for these novel catalysts is promising, the required metal load is inconveniently high. A considerable reduction in the Pt charge is obtained by adding Re to the carbon support, but the noble metal content remains high [36].

Finally, with a similar support, Kim et al. [37] developed new catalysts with 3 wt.% Pt, modified with Fe in different atomic ratios (Table 4). The catalysts are an improvement in relation to the previously discussed examples. They have a superior conversion capacity and higher H_2 yield. However, the authors did not report the coke content of catalyst after the experiments. This report had very good results though the Pt content (3 wt.%) is higher than ours. It is also important to note that Fe greatly improves the conversion and H_2 yield, in a similar way as Ni and Co did in the present work.

4. Conclusions

At the APR reaction, conditions of this work Pt/Al_2O_3 catalysts prepared by incipient wetness impregnation (IWI) show a hydrogen yield of about 15.2%. The addition of 3% Ni or Co and the use of a different method of metal addition (urea matrix combustion, UMC) produce catalysts that have a higher yield to hydrogen and a higher stability and a lower selectivity to coke and methane. Particularly, the addition of Co by UMC increases the hydrogen yield by 50% in relation to the standard Pt/Al_2O_3 catalyst, while keeping similar hydrogen selectivity and a much lower selectivity to methane. The addition of Ni by UMC increases the hydrogen yield by 75% in comparison to the standard Pt/Al_2O_3 catalyst but increases both the methanation and coking activities.

The simultaneous use of the UMC method and Ni and Co promotion enabled the synthesis of APR catalysts that had a lower metal content than those reported in the literature, but a similar or better activity level.

The decrease of the selectivity to the undesired products such as coke and methane enabled an increase of the conversion by a factor of two and of the hydrogen yield by a factor of 1.5.

A comparison with published results indicates that catalysts of other authors obtained similar or better results than ours, but with the use of higher metal contents or more expensive supports. In some cases, their experiments were carried out with diluted solutions of ethylene glycol or higher reaction temperatures and pressures, conditions that are associated with higher operation costs.

In summary, APR catalyst of low noble metal content and hence of low cost can be obtained by using the UMC method to incorporate Ni or Co promoters to alumina supported Pt catalysts. These catalysts show promising catalytic properties for the improved production of H_2 by APR of biomass related feedstocks.

Data Availability

The data used to support the findings of this study are available from the corresponding author upon request.

Conflicts of Interest

There are no conflicts to declare.

Acknowledgments

The authors thank Sasol for the donation of alumina used in this paper. The authors also thank the financial support of CONICET (PIP Grant 2014-560), Universidad Nacional delLitoral (CAI+D Grant 2016-084), and ANPCyT (PICT Grant 2013–3217).

References

[1] G. J. Antos, A. M. Aitani, and J. M. Parera, *Catalytic Naphtha Reforming Science and Technology*, Marcel Dekker, Inc., New York, NY, USA, 1995.

[2] M. W. Twigg, *Catalyst Handbook*, Wolfe Publishing Ltd., London, UK, 1989.

[3] X. Zhang, Q. Zhang, T. Wang, B. Li, Y. Xu, and L. Ma, "Efficient upgrading process for production of low quality fuel from bio-oil," *Fuel*, vol. 179, pp. 312–321, 2016.

[4] X. Zhang, Q. Zhang, T. Wang, L. Ma, Y. Yu, and L. Chen, "Hydrodeoxygenation of lignin-derived phenolic compounds to hydrocarbons over Ni/SiO_2–ZrO_2 catalysts," *Bioresource Technology*, vol. 134, pp. 73–80, 2013.

[5] X. Zhang, T. Wang, L. Ma, Q. Zhang, X. Huang, and Y. Yu, "Production of cyclohexane from lignin degradation compounds over Ni/ZrO_2–SiO_2 catalysts," *Applied Energy*, vol. 112, pp. 533–538, 2013.

[6] D. J. Wuebbles and A. K. Jain, "Concerns about climate change and the role of fossil fuel use," *Fuel Processing Technology*, vol. 71, pp. 99–119, 2001.

[7] T. Nozawa, A. Yoshida, S. Hikichi, and S. Naito, "Effects of Re addition upon aqueous phase reforming of ethanol over TiO_2 supported Rh and Ir catalysts," *International Journal of Hydrogen Energy*, vol. 40, pp. 4129–4140, 2015.

[8] G. W. Huber and J. A. Dumesic, "An overview of aqueous-phase catalytic processes for production of hydrogen and alkanes in a biorefinery," *Catalysis Today*, vol. 111, pp. 119–132, 2006.

[9] I. Coronado, M. Stekrova, M. Reinikainen, P. Simell, L. Lefferts, and J. Lehtonen, "A review of catalytic aqueous-phase reforming of oxygenated hydrocarbons derived from biorefinery water fractions," *International Journal of Hydrogen Energy*, vol. 41, pp. 11003–11032, 2016.

[10] R. R. Davda, J. W. Shabaker, G. W. Huber, R. D. Cortright, and J. A. Dumesic, "A review of catalytic issues and process conditions for renewable hydrogen and alkanes by aqueous-phase reforming of oxygenated hydrocarbons over supported metal catalysts," *Applied Catalysis B: Environmental*, vol. 56, pp. 171–186, 2005.

[11] J. W. Shabaker, G. W. Huber, and J. A. Dumesic, "Aqueous-phase reforming of oxygenated hydrocarbons over Sn-modified Ni catalysts," *Journal of Catalysis*, vol. 222, pp. 180–191, 2004.

[12] G. W. Huber, J. W. Shabaker, S. T. Evans, and J. A. Dumesic, "Aqueous-phase reforming of ethylene glycol over supported Pt and Pd bimetallic catalysts," *Applied Catalysis B: Environmental*, vol. 62, pp. 226–235, 2006.

[13] A. Martinez and G. Prieto, "Breaking the dispersion-reducibility dependence in oxide-supported cobalt nanoparticles," *Journal of Catalysis*, vol. 245, no. 2, pp. 470–476, 2007.

[14] S. L. González-Cortés, T. Xiao, and M. Green, *Scientific Bases for the Preparation of Heterogeneous Catalysts*, Elsevier, Oxford, UK, 1st edition, 2006.

[15] S. L. González-Cortés and F. E. Imbert, "Fundamentals, properties and applications of solid catalysts prepared by solution combustion synthesis (SCS)," *Applied Catalysis A: General*, vol. 452, pp. 117–131, 2013.

[16] G. Xanthopoulou and G. Vekinis, "Investigation of catalytic oxidation of carbon monoxide over a Cu–Cr-oxide catalyst made by self-propagating high-temperature synthesis," *Applied Catalysis B: Environmental*, vol. 19, pp. 37–44, 1998.

[17] A. Varma, A. S. Mukasyan, A. S. Rogachev, and K. V. Manukyan, "Solution combustion synthesis of nanoscale materials," *Chemical Reviews*, vol. 116, no. 23, pp. 14493–14586, 2016.

[18] M. Boudart, A. Aldag, J. E. Benson, N. A. Dougharty, and C. G. Harkins, "On the specific activity of platinum catalysts," *Journal of Catalysis*, vol. 6, no. 1, pp. 92–99, 1966.

[19] R. R. Davda, J. W. Shabaker, G. W. Huber, R. D. Cortright, and J. A. Dumesic, "Aqueous-phase reforming of ethylene glycol on silica-supported metal catalysts," *Applied Catalysis B: Environmental*, vol. 43, no. 1, pp. 13–26, 2003.

[20] R. D. Cortright, R. R. Davda, and J. A. Dumesic, "Hydrogen from catalytic reforming of biomass-derived hydrocarbons in liquid water," *Nature*, vol. 418, no. 6901, pp. 964–967, 2002.

[21] E. Ko, E. Park, K. W. Seo, H. C. Lee, D. Lee, and S. Kim, "Pt–Ni/γ-Al_2O_3 catalyst for the preferential CO oxidation in the hydrogen stream," *Catalysis Letters*, vol. 110, pp. 275–279, 2006.

[22] Joint Committee on Powder Diffraction Standards (JCPDS) file No. 86–1410.

[23] K. Persson, A. Ersson, S. Colussi, A. Trovarelli, and S. G. Järas, "Catalytic combustion of methane over bimetallic Pd–Pt catalysts: the influence of support materials," *Applied Catalysis B: Environmental*, vol. 66, no. 3-4, pp. 175–185, 2006.

[24] N. Luo, K. Ouyang, F. Cao, and T. Xiao, "Hydrogen generation from liquid reforming of glycerin over Ni–Co bimetallic catalyst," *Biomass Bioenergy*, vol. 34, pp. 489–495, 2010.

[25] M. C. Rangel, L. S. Carvalho, P. Reyes, J. M. Parera, and N. S. Fıgoli, "*n*-octane reforming over alumina-supported Pt, Pt–Sn and Pt–W catalysts," *Catalysis Letters*, vol. 64, pp. 171–178, 2000.

[26] C. Hwang and C. Yeh, "Platinum-oxide species formed by oxidation of platinum crystallites supported on alumina," *Journal of Molecular Catalysis A: Chemical*, vol. 112, no. 2, pp. 295–302, 1996.

[27] L. F. Liotta, G. Pantaleo, A. Macaluso, G. Di Carlo, and G. Deganello, "CoO_x catalysts supported on alumina and alumina-baria: influence of the support on the cobalt species and their activity in NO reduction by C3H6 in lean conditions," *Applied Catalysis A: General*, vol. 245, no. 1, pp. 167–177, 2003.

[28] S. Rane, Ø. Borg, J. Yang, E. Rytter, and A. Holmen, "Effect of alumina phases on hydrocarbon selectivity in Fischer–Tropsch synthesis," *Applied Catalysis A: General*, vol. 388, pp. 160–167, 2010.

[29] D. Nabaho, J. W. Niemantsverdriet, M. Claeys, and E. van Steen, "Hydrogen spillover in the Fischer–Tropsch synthesis: an analysis of platinum as a promoter for cobalt–alumina catalysts," *Catalysis Today*, vol. 261, pp. 17–27, 2016.

[30] M. El Doukkali, A. Iriondo, P. L. Arias et al., "A comparison of sol–gel and impregnated Pt or/and Ni based γ-alumina catalysts for bioglycerol aqueous phase reforming," *Applied Catalysis B: Environmental*, vol. 125, pp. 516–529, 2012.

[31] J. Li, W. P. Tian, X. Wang, and L. Shi, "Nickel and nickel–platinum as active and selective catalyst for the maleic anhydride hydrogenation to succinic anhydride," *Chemical Engineering Journal*, vol. 175, pp. 417–422, 2011.

[32] W. Nabgan, T. Amran, T. Abdullah et al., "Hydrogen production from catalytic steam reforming of phenol with bimetallic nickel-cobalt catalyst on various supports," *Applied Catalysis A: General*, vol. 527, pp. 161–170, 2016.

[33] D. J. M. de Vlieger, B. L. Mojet, L. Lefferts, and K. Seshan, "Aqueous Phase Reforming of ethylene glycol – Role of intermediates in catalyst performance," *Journal of Catalysis*, vol. 292, pp. 239–245, 2012.

[34] H. D. Kim, H. J. Park, T. W. Kim et al., "Hydrogen production through the aqueous phase reforming of ethylene glycol over supported Pt-based bimetallic catalysts," *International Journal of Hydrogen Energy*, vol. 37, pp. 8310–8317, 2012.

[35] H. D. Kim, T. W. Kim, H. J. Park et al., "Hydrogen production via the aqueous phase reforming of ethylene glycol over platinum-supported ordered mesoporous carbon catalysts: effect of structure and framework-configuration," *International Journal of Hydrogen Energy*, vol. 37, pp. 12187–2197, 2012.

[36] H. D. Kim, H. J. Park, T. W. Kim et al., "The effect of support and reaction conditions on aqueous phase reforming of polyol over supported Pt–Re bimetallic catalysts," *Catalysis Today*, vol. 185, pp. 73–80, 2012.

[37] M. C. Kim, T. W. Kim, H. J. Kim, C. U. Kim, and J. W. Bae, "Aqueous phase reforming of polyols for hydrogen production using supported PtFe bimetallic catalysts," *Renewable Energy*, vol. 95, pp. 396–403, 2016.

[38] T. W. Kim, H. D. Kim, K. E. Jeong et al., "Catalytic production of hydrogen through aqueous-phase reforming over platinum/ordered mesoporous carbon catalysts," *Green Chemistry*, vol. 13, pp. 1718–1728, 2011.